Continuous quantum measurement of a Bose-Einstein condensate: A stochastic Gross-Pitaevskii equation

Diego A. R. Dalvit,[1] Jacek Dziarmaga,[1,2] and Roberto Onofrio[1,3,4]
Los Alamos National Laboratory, Los Alamos, New Mexico 87545
[2]*Intytut Fizyki Uniwersytetu Jagiellońskiego, ul. Reymonta 4, 30-059 Kraków, Poland*
[3]*Dipartimento di Fisica "G. Galilei," Università di Padova, Padova 35131, Italy*
[4]*INFM, Unità di Roma 1 and Center for Statistical Mechanics and Complexity, Rome 00185, Italy*
(Received 17 December 2001; published 19 April 2002)

We analyze the dynamics of a Bose-Einstein condensate undergoing a continuous dispersive imaging by using a Lindblad operator formalism. Continuous strong measurements drive the condensate out of the coherent-state description assumed within the Gross-Pitaevskii mean-field approach. Continuous weak measurements allow us instead to replace, for time scales short enough, the exact problem with its mean-field approximation through a stochastic analog of the Gross-Pitaevskii equation. The latter is used to show the unwinding of a dark soliton undergoing a continuous imaging.

DOI: 10.1103/PhysRevA.65.053604 PACS number(s): 03.75.Fi, 05.30.Jp, 05.40.−a

I. INTRODUCTION

The interplay between quantum and classical descriptions of the physical world and the role of the measurement process are still at the heart of the understanding of quantum mechanics [1]. The related theoretical debate has been greatly enriched in recent decades by the realization of new experimental techniques aimed at producing quantum states without classical analog, such as entangled or squeezed states, or exploring phenomena which are intrinsically quantum-mechanical, such as quantum jumps. All this occurred also keeping in mind practical implications, such as the improvement of the sensitivity of various devices operating at or near the quantum limit [2,3].

Recently, the production of a novel state of matter—Bose-Einstein condensates of dilute atomic gases—has opened a new road to explore macroscopic quantum phenomena with the precision characteristic of atomic physics [4]. Bose-Einstein condensates are naturally produced by cooling down atomic gases at ultralow temperature with the phase transition occurring in the 100 nK–1 μK temperature range, i.e., when the thermal de Broglie wavelength becomes comparable to the average spacing between the atoms of a dilute (peak density $10^{13}-10^{15}$ atoms/cm^3) trapped gas. Usually samples of Bose-Einstein condensates are made by 10^3-10^8 atoms in the case of alkali-metal species [4], and 10^9 or more in the case of hydrogen [5]. Their intrinsically small heat capacity does not allow for a direct manipulation and probing with material samples, such as microtips or nanostructures, since the thermal contact with the latter will induce a sudden evaporation of the Bose sample. Thus, manipulation and probing of Bose-Einstein condensates has been achieved so far only by using light beams. These probes can be classified according to the resonant or nonresonant nature of their interaction with the measured atomic sample. In the former case, the condensate interacts with a laser beam resonant (or close to resonant) with a selected atomic transition. The output beam is attenuated proportionally to the optical thickness of the condensate (also called column density), i.e., the condensate density integrated along the line of sight of the impinging beam. The absorption of the photons leads to a recoil of the atoms, which strongly perturbs the condensate. For typical values of intensity and duration of the probe light, the condensate is strongly heated and a new replica has to be produced to further study its dynamics. From the viewpoint of quantum measurement theory, this measurement is of type II since it destroys the state of the observed system and forbids the study of the dynamics of a single quantum system [6]. An alternative technique, called dispersive imaging, allows for repeated measurements on a Bose-Einstein condensate and, as an extreme case, its continuous monitoring. In this measurement scheme, off-resonance light is scattered by the condensate, thereby locally inducing optical phase shifts which can be converted into light intensity modulations by homodyne or heterodyne techniques, for instance by using phase contrast [7], modulation spectroscopy [8,9], and interference [10] techniques (for a similar nondestructive imaging technique based upon polarimetry, see [11]). Since the laser beam is off-resonant, the absorption rate is small and the heating of the condensate is accordingly small. Thus, multiple shots of the same condensate can be taken—a type-I measurement in the quantum measurement theory language—allowing the study of the dynamics on the same sample. This has allowed us to overcome the unavoidable shot-to-shot fluctuations always present in the production of different samples of Bose-Einstein condensates. Several phenomena whose observations are based upon imaging the condensate at high accuracy, such as its formation in nonadiabatic conditions [12], short- [13] and long- [14] wavelength collective excitations, superfluid dynamics [15], and vortices formation and decay [16,17], can be successfully studied with this technique.

The repeated nondestructive monitoring lends itself to another question: *is the measurement process influencing the dynamics of the condensate?* Answers to this question are important also for disentangling the intrinsic condensate dynamics from the artifacts induced by the underlying measurement process. As we will see in this paper, the effect of the measurement can also be intentionally amplified to allow

for unusual manipulation of the condensate itself. Dispersive imaging, in its more idealized form, is preserving the number of atoms and therefore represents a particular example of quantum nondemolition (QND) measurement [2,18,19]. We know that even quantum nondemolition measurements affect the state of the observed system, their unique feature being that the nondemolitive observable maintains the same *average* value, albeit the probability distribution of its outcome can be affected as well as the average values of all the conjugate observables. Thus, we do expect that during the nondemolitive measurement of the condensate atom number there will be a measurement-induced nontrivial dynamics for both the variance of the monitored observable and the average values of all conjugate observables. Besides gaining insight into the dynamics of the measurement process, our model allows for a description of the *irreversible* driving of the condensate toward nonclassical states.

In this paper, we try to answer the question formulated above by building a realistic model for dispersive measurements of the condensate, extending the results reported in [20] to the weak measurement regime. The plan of the paper is as follows. In Sec. II, we introduce the dispersive coupling between atoms and light and derive the reduced master equation for the Bose condensate tracing out the variables of the electromagnetic field degrees of freedom. Under controllable approximations, we obtain a Lindblad equation which allows us to estabilish the rates for phase diffusion and depletion of the condensate during the dispersive imaging. In Sec. III, we unravel the Lindblad equation by neglecting the depletion term, obtaining a stochastic differential equation that, in the unmeasured case, corresponds to the description of a single *N*-body wave function. A solution of the stochastic *N*-body equation is discussed in the limit of strong continuous measurement, leading to the squeezing of number fluctuations; the main result is described in [20]. In the opposite limit of weak measurement and for an initial mean-field state, this stochastic equation becomes the stochastic counterpart of the Gross-Pitaevskii equation, as discussed in Sec. IV. Its limit of validity is discussed in Sec. V by comparing its evolution for various parameters versus the exact evolution in the simple situation of a two-mode system schematizing a condensate in a double well potential. This allows us to analyze, in Sec. VI, the effect of the measurement on the evolution of a condensate initially prepared in a soliton state. More general considerations on the potentiality of such an approach and its consequences are finally outlined in the conclusions.

II. MASTER EQUATION FOR DISPERSIVE IMAGING OF A BOSE CONDENSATE

Our main goal in this section is to include the atom-photon interaction present in the dispersive imaging of a Bose-Einstein condensate into its intrinsic dynamics. First attempts in this direction have been discussed in the prototypical situation of a two-mode condensate in [21,22]. Let us start the analysis with the effective interaction Hamiltonian between the off-resonant photons and the atoms, written as

$$H_{\rm int}=\frac{\epsilon_0\chi_0}{2}\int d^3x\, n(\mathbf{x}):\mathbf{E}^2:, \tag{1}$$

where n is the density operator of the atomic vapor and $\mathbf{E}$ is the electric field due to the intensity I of the incoming light. The coefficient χ_0 represents the effective electric susceptibility of the atoms defined as $\chi_0=\lambda^3\delta/2\pi^2(1+\delta^2)$, where we have introduced the light wavelength λ and the light detuning measured in half-linewidths $\Gamma/2$ of the atomic transition, $\delta=(\omega-\omega_{\rm at})/(\Gamma/2)$.

We express the electric field in terms of creation and annihilation operators. In the Coulomb gauge, it takes the form

$$\mathbf{E}(\mathbf{x},t)=i\sum_{\mathbf{k}}\sqrt{\frac{\hbar\omega_{\mathbf{k}}}{2\epsilon_0 L^3}}[a_{\mathbf{k}}\exp(-i\omega_{\mathbf{k}}t+i\mathbf{k}\cdot\mathbf{x}) - a_{\mathbf{k}}^{\dagger}\exp(i\omega_{\mathbf{k}}t-i\mathbf{k}\cdot\mathbf{x})], \tag{2}$$

where $\omega_{\mathbf{k}}=c|\mathbf{k}|$, $[a_{\mathbf{k}},a_{\mathbf{k}'}^{\dagger}]=\delta_{\mathbf{k},\mathbf{k}'}$, and L^3 is the quantization volume. Equation (1) allows us to write the reduced master equation for the atomic degrees of freedom by a standard technique, i.e., by tracing out the photon degrees of freedom [23]. The decoupling between the two relevant time scales for the photons (settled by the lifetime of spontaneous emission, of order of tens ns) and for the atoms (related to the oscillation period in the trapping potential, of the order of ms), allows us to use the Born-Markov approximation. Thus we get the master equation for the reduced density matrix ρ of the condensate that, in the interaction picture, is written as

$$\frac{d\rho}{dt}=\frac{i}{\hbar}{\rm Tr}_{\rm R}[\rho(t)\otimes\rho_{\rm R}(t),H_{\rm int}]-\frac{1}{\hbar^2}{\rm Tr}_{\rm R}\times\left[H_{\rm int}(t),\left[\int_{-\infty}^{t}dt' H_{\rm int}(t'),\rho(t)\otimes\rho_{\rm R}(t)\right]\right]. \tag{3}$$

The last term on the right-hand side contains two different contributions both of Lindblad type, $L_1\rho$ and $L_2\rho$. As we will see soon, the former preserves the number of atoms in the condensate and is responsible for phase-diffusion phenomena, while the latter changes the number of atoms leading to its depletion.

Let us first concentrate on phase diffusion, which is a number-conserving mechanism. To calculate it, we insert the interaction Hamiltonian into the last term of Eq. (3), with n the condensate density operator. By introducing the Fourier transform of the density operator such that

$$n(\mathbf{x})=\sum_{\mathbf{q}}\frac{\tilde{n}(\mathbf{q})}{\sqrt{L^3}}\exp(i\mathbf{q}\cdot\mathbf{x}), \tag{4}$$

we obtain

$$L_1\rho=\frac{\pi\chi_0^2}{2L^3c}\sum_{\mathbf{k},\mathbf{p}}\sqrt{\omega_{\mathbf{k}}\omega_{\mathbf{p}}}\delta(k-p)\sum_{\mathbf{k}',\mathbf{p}'}\sqrt{\omega_{\mathbf{k}'}\omega_{\mathbf{p}'}}e^{ict(k'-p')}$$
$$\times[\tilde{n}(\mathbf{k}'-\mathbf{p}')\tilde{n}(\mathbf{k}-\mathbf{p})\rho\langle a_{\mathbf{k}'}^\dagger a_{\mathbf{p}'}a_{\mathbf{k}}^\dagger a_{\mathbf{p}}\rangle$$
$$-\tilde{n}(\mathbf{k}'-\mathbf{p}')\rho\tilde{n}(\mathbf{k}-\mathbf{p})\langle a_{\mathbf{k}}^\dagger a_{\mathbf{p}}a_{\mathbf{k}'}^\dagger a_{\mathbf{p}'}\rangle$$
$$-\tilde{n}(\mathbf{k}-\mathbf{p})\rho\tilde{n}(\mathbf{k}'-\mathbf{p}')\langle a_{\mathbf{k}'}^\dagger a_{\mathbf{p}'}a_{\mathbf{k}}^\dagger a_{\mathbf{p}}\rangle$$
$$+\rho\tilde{n}(\mathbf{k}-\mathbf{p})\tilde{n}(\mathbf{k}'-\mathbf{p}')\langle a_{\mathbf{k}}^\dagger a_{\mathbf{p}}a_{\mathbf{k}'}^\dagger a_{\mathbf{p}'}\rangle], \quad (5)$$

where $\langle\ \rangle=\mathrm{Tr}_R[\rho_R\cdots]$. The photons are assumed to be in a coherent plane-wave state with momentum along the impinging direction, corresponding to a wave vector $\mathbf{k}=k_0\hat{z}$ orthogonal to the imaging plane x-y. Hence

$$\langle a_{\mathbf{k}'}^\dagger a_{\mathbf{p}}\rangle=\frac{L^3 I}{c^2\hbar k_0}\delta_{\mathbf{k}',\mathbf{p}}\delta_{\mathbf{p},\mathbf{k}_0}, \quad (6)$$

where we have written the mean numbers of photons in mode k_0 in terms of the intensity of the incoming beam. Expressing the expectation values in normal ordering and using the fact that phase-diffusion processes conserve the number of bosons in the condensate, it is possible to show that all normal ordered expectation values involving four operators cancel exactly, obtaining

$$L_1\rho=\frac{\pi\chi_0^2 I k_0}{2\hbar c}\left(\frac{L}{2\pi}\right)^3$$
$$\times\int d^3k\ \delta(|\mathbf{k}+\mathbf{k}_0|-k_0)[\tilde{n}(-\mathbf{k}),[\tilde{n}(\mathbf{k}),\rho]], \quad (7)$$

where we have used the continuum limit $\Sigma_{\mathbf{k}}\rightarrow(L/2\pi)^3\int d^3k$. Unless tomographic techniques are used, as, for instance in [24], the image results from a projection of the condensate onto the x-y plane, by integrating along the z direction. This requires us to project the dynamics of the condensate into the imaging plane. In order to write a closed 2D master equation to describe the x-y dynamics, we assume the condensate wave function to be factorizable as $\psi(x,y,z)=\phi(x,y)\Lambda(z)$. Such factorization holds if the confinement in the z direction is strong enough to make the corresponding mean-field energy negligible with respect to the energy quanta of the confinement, i.e., $\hbar\omega_z\gg g\tilde{\rho}$, where $g=4\pi\hbar^2 a/m$, with a the s-wave scattering length, $\tilde{\rho}$ the condensate density, and ω_z the angular frequency of the confinement harmonic potential along the z direction, as recently demonstrated experimentally in [25]. We write $\tilde{n}(\mathbf{k})=\tilde{n}(\mathbf{k}_\perp)\tilde{n}(k_z)$ and we will use a Gaussian ansatz for the density profile along the z direction, namely

$$\tilde{n}(k_z)=\sqrt{\frac{2\pi}{L}}\exp\left(-\frac{\xi^2k_z^2}{2}\right), \quad (8)$$

where ξ is the length scale of the condensate in the z direction, which is the width of the Gaussian state $\Lambda(z)$ under the above-mentioned approximation. The effective 2D nonlinear coupling strength is $g_{2D}=g\int dz|\Lambda(z)|^4=g\sqrt{\pi}/\xi$. Consequently,

$$L_1\rho=\frac{\pi\chi_0^2 I k_0}{2\hbar c}\left(\frac{L}{2\pi}\right)^2\int d^2k_\perp[\tilde{n}(-\mathbf{k}_\perp),[\tilde{n}(\mathbf{k}_\perp),\rho]]\left(\frac{L}{2\pi}\right)$$
$$\times\int dk_z\tilde{n}^2(k_z)\delta(|\mathbf{k}+\mathbf{k}_0|-k_0). \quad (9)$$

By assuming that the typical length of the BEC in the z direction is much larger than the wavelength of the incoming laser, i.e., $\xi\gg\lambda$, we can calculate the value of the last integral, and it is equal to $\exp(-\xi^2\mathbf{k}_\perp^4/4k_0^2)$. Our final result for the phase-diffusion contribution to the reduced master equation in the imaging plane is written as

$$L_1\rho=\int d^2r_1\int d^2r_2K(\mathbf{r}_1-\mathbf{r}_2)[n(\mathbf{r}_1),[n(\mathbf{r}_2),\rho]], \quad (10)$$

where $n(\mathbf{r})=\Psi^\dagger\Psi(\mathbf{r})$ is the 2D density operator and K is the measurement kernel,

$$K(\mathbf{r})=\frac{\pi\chi_0^2k_0I}{2\hbar c}\int d^2k\exp(-\xi^2k^4/4k_0^2+i\mathbf{k}\cdot\mathbf{r}). \quad (11)$$

Equation (10) preserves the total number of atoms and corresponds to a quantum nondemolition coupling between the atom and the optical fields [21,22,26–28]. If the measurement kernel were a local one, $K(\mathbf{r}_1-\mathbf{r}_2)\simeq\delta(\mathbf{r}_1-\mathbf{r}_2)$, Eq. (10) would reduce to a Lindblad equation for the measurement of an infinite number of densities $n(\mathbf{r})$. This assumes that no spatial correlation is established by the photon detection. However, the ultimate resolution limit in the imaging system depends on the photon wavelength, regardless of the pixel density of the detecting camera. The resolution length scale follows from Eq. (11) as a width of the kernel,

$$\Delta r=(2\pi^2\xi/k_0)^{1/2}=(\pi\xi\lambda)^{1/2}, \quad (12)$$

the geometrical average of the light wavelength and the condensate thickness ξ. Equation (10) can then be rewritten as $L_1\rho=\gamma_1[n,[n,\rho]]$, where γ_1 is the phase-diffusion rate, given by

$$\gamma_1=\frac{\pi\chi_0^2k_0I}{2\hbar c}\int d^2k|\phi(\mathbf{k})|^2|\phi(-\mathbf{k})|^2\exp\left(-\frac{\xi^2k^4}{4k_0^2}\right). \quad (13)$$

We estimate its magnitude assuming a Gaussian profile in the x-y plane, i.e., $|\phi(\mathbf{k})|^2=\exp(-\alpha^2k^2/2)$, obtaining

$$\gamma_1=\frac{\pi^{5/2}\chi_0^2k_0^2I}{2\hbar c\xi}\exp\left(\frac{\alpha^4k_0^2}{\xi^2}\right)\left[1-\mathrm{erf}\left(\frac{\alpha^2k_0}{\xi}\right)\right]\approx\frac{\pi^2\chi_0^2k_0I}{2\hbar c\alpha^2}, \quad (14)$$

where the last step holds for a well-localized condensate, i.e., $\alpha^2k_0/\xi\gg1$.

Let us now calculate the depletion contribution to the master equation for the condensate. We split the field annihilation operator into a term describing the condensate and another associated to the noncondensed particles, i.e., $\psi = \psi_C + \psi_{NC}$. We shall assume that the noncondensed particles belong to the continuum, so that their spectrum is that of a free particle $\hbar\Omega_{\mathbf{q}} = \hbar^2 q^2/2m$. Indeed, photons have large momenta with respect to the momenta of trapped atoms, so even if a small percentage of the photon momentum is absorbed by the atom, the atom is promoted into a high-energy, unbounded state. Let us expand both field operators in terms of annihilation operators as

$$\psi_C(\mathbf{x},t) = b_C \phi_C(\mathbf{x},t),$$

$$\psi_{NC}(\mathbf{x},t) = \frac{1}{\sqrt{L^3}} \sum_{\mathbf{q}} \exp(-i\Omega_{\mathbf{q}} t + i\mathbf{q}\cdot\mathbf{x}) b_{\mathbf{q}}, \qquad (15)$$

where ϕ_C is the condensate wave function. We get

$$\begin{aligned} L_2\rho = \frac{\pi\chi_0^2}{8cL^6} \sum_{\mathbf{kpq}} \sqrt{\omega_{\mathbf{k}}\omega_{\mathbf{p}}} \sum_{\mathbf{k}'\mathbf{p}'\mathbf{q}'} \sqrt{\omega'_{\mathbf{k}}\omega'_{\mathbf{p}}}\,\delta(\Omega_{\mathbf{q}'} - ck' + cp') \\ \times \{\exp[it(\Omega_{\mathbf{q}} - ck + cp)]\,\tilde{\phi}_C(q+p-k)\,\tilde{\phi}_C^*(q'+p'-k')\,\mathrm{Tr}_R[a_{\mathbf{p}}^\dagger a_{\mathbf{k}} b_{\mathbf{q}}^\dagger b_C, [a_{\mathbf{k}'}^\dagger a_{\mathbf{p}'} b_{\mathbf{q}'} b_C^\dagger, \rho]] \\ + \exp[-it(\Omega_{\mathbf{q}} - ck + cp)]\,\tilde{\phi}_C^*(q+p-k)\,\tilde{\phi}_C(q'+p'-k')\,\mathrm{Tr}_R[a_{\mathbf{k}}^\dagger a_{\mathbf{p}} b_{\mathbf{q}} b_C^\dagger, [a_{\mathbf{p}'}^\dagger a_{\mathbf{k}'} b_{\mathbf{p}'}^\dagger b_C, \rho]]\}. \end{aligned} \qquad (16)$$

Here the trace is taken over the reservoir of the condensate, which in this case consists of the noncondensed particles and the photons. The above expression contains depletion processes, in which a photon interacts with a particle in the condensate and, as a result, that particle is kicked out of the condensate. It also contains feeding processes, in which the reverse mechanism may take place. When one assumes that in the initial state of the noncondensate the plane waves are empty, only the depletion process is relevant. In this hypothesis, we find

$$L_2\rho = \gamma_2(-b_C\rho b_C^\dagger + \tfrac{1}{2}\{b_C^\dagger b_C, \rho\}), \qquad (17)$$

where γ_2 is the depletion rate,

$$\begin{aligned} \gamma_2 = \frac{\pi\chi_0^2 I}{4\hbar c L^3}\left(\frac{L}{2\pi}\right)^6 \int d^3p\, d^3q\, \omega_{\mathbf{p}} |\tilde{\phi}_C(\mathbf{q}+\mathbf{p}-\mathbf{k}_0)|^2 \\ \times \delta(\Omega_{\mathbf{q}} - ck_0 + cp). \end{aligned} \qquad (18)$$

We evaluate γ_2 in the thick condensate limit ($\xi \gg k_0^{-1}$) by approximating $|\tilde{\phi}_C(\mathbf{q}+\mathbf{p}-\mathbf{k}_0)|^2 \approx (2\pi/L)^3 \delta(\mathbf{q}+\mathbf{p}-\mathbf{k}_0)$, and then, by using the fact that $\Omega_{\mathbf{q}} \ll ck_0$, we obtain

$$\gamma_2 = \frac{\chi_0^2 k_0^3 I}{8\pi\hbar c}. \qquad (19)$$

Similar relationships have been obtained in other contexts, namely the nondestructive monitoring of two-mode systems with either an internal [21] or external [22] degree of freedom, the dynamics of an atom laser subjected to feedback [29], and the multimode imaging analyzed in [28]. In all these cases, despite the quite different physical setups, phase-diffusion coefficients in the corresponding Lindblad master equations present the same scaling on the common parameters, such as the light intensity and its detuning with respect to the atomic transition. From Eqs. (14) and (19), we see that the depletion rate is much bigger than the phase-diffusion rate $\gamma_2/\gamma_1 = \alpha^2/\pi\lambda^2 \simeq 10^2 \gg 1$, in accordance with Ref. [28]. We estimate the magnitude of both rates using the following parameters for the condensate and its imaging, relevant for the case of ^{87}Rb: $\lambda = 780$ nm, $\chi_0 = 10^{-23}$ m^3, laser intensity $I = 10^{-4}$ mW/cm^2, and a typical size in the x-y plane of $\alpha = 10$ μm. Then $\gamma_1 = 10^{-6}$ s^{-1} and $\gamma_2 = 10^{-5}$ s^{-1}, corresponding to phase-diffusion and depletion times of $t_1 = \gamma_1^{-1} = 10^5$ s and $t_2 = \gamma_2^{-1} = 10^4$ s, respectively. Although the depletion rate is larger than the phase-diffusion rate, this last process can dominate because of their different scaling with the total number of condensed particles in the master equation. Indeed, the first is linear in N (as any single-particle scattering rate), whereas the second one is quadratic (due to the double commutator for n present in the phase-diffusion Lindblad term), so for a large number of particles (such as $N = 10^7$), phase diffusion occurs on a faster time scale than depletion. This also confirms the conventional wisdom that macroscopic coherent states are more fragile with respect to decoherence. Moreover, in various situations such as imaging of condensates with nontrivial topological patterns, depletion acts uniformly just scaling the atomic density while phase diffusion can change the pattern, as we will see soon. For these reasons, we will focus in the following on the phase-diffusion contribution alone.

III. STRONG MEASUREMENT: MEASUREMENT-INDUCED NUMBER SQUEEZING

We will consider in the following the effect of strong measurements on the quantum state of the condensate. This has already been described in detail elsewhere [20], thus here

we only summarize the main results and their link to the following considerations. By neglecting the depletion term, the master equation for the condensate takes the form $\dot{\rho}=(-i/\hbar)[H,\rho]-L_1\rho$. This equation preserves the total number of atoms in the condensate and corresponds to a quantum nondemolition measurement of the atomic density via the optical fields. In order to get an insight into the equation, we introduce a two-dimensional lattice with the lattice constant set by the kernel resolution Δr. In this way, we get

$$\frac{d\rho}{dt}=-\frac{i}{\hbar}\left[-\hbar\omega\sum_{\langle k,l\rangle}\Psi_k^\dagger\Psi_l+V,\rho\right]-S\sum_l[n_l,[n_l,\rho]]. \tag{20}$$

Here Ψ_l is an annihilation operator and $n_l=\Psi_l^\dagger\Psi_l$ is the number operator at a lattice site l. The frequency of hopping between any nearest-neighbor sites $\langle k,l\rangle$ is $\omega\approx\hbar/2m\Delta r^2$, which is $\hbar^{-1}$ times the characteristic kinetic energy. The potential-energy operator is $V=\Sigma_l(U_l n_l+Gn_l^2)$, where U_l is the trapping potential and $G=g_{2D}/\Delta r^2$. The effective measurement strength is $S\approx\int d^2rK(\mathbf{r})/\Delta r^2=(2\pi/\Delta r)^2(\pi\chi_0^2k_0I/2\hbar c)$. In order to solve this equation, we use an unraveling in terms of pure states $|\Psi\rangle$ such that $\rho=\overline{|\Psi\rangle\langle\Psi|}$, where the overline denotes the average over the unraveling stochastic realizations. The pointer states of Eq. (20) are not changed by the chosen unraveling [30]. The pure states can be expanded in a Fock basis per site, $|\Psi\rangle=\Sigma_{\{N_l\}}\psi_{\{N_l\}}|\{N_l\}\rangle$, and the amplitudes $\psi_{\{N_l\}}$ satisfy the following stochastic Schrödinger equation (written in the Stratonovich convention):

$$\frac{d}{dt}\psi_{\{N_l\}}=-\frac{i}{\hbar}\sum_{\{N_l'\}}h_{\{N_l,N_l'\}}\psi_{\{N_l'\}}-\frac{i}{\hbar}V_{\{N_l\}}\psi_{\{N_l\}}+\psi_{\{N_l\}}\sum_l[-S(N_l-n_l)^2+S\sigma_l^2+(N_l-n_l)\theta_l], \tag{21}$$

where the homodyne noises have averages $\overline{\theta_l(t)}=0$ and $\overline{\theta_{l_1}(t_1)\theta_{l_2}(t_2)}=2S\delta_{l_1,l_2}\delta(t_1-t_2)$. Here $n_l=\Sigma_{\{N_l\}}N_l|\psi_{\{N_l\}}|^2$, $\sigma_l^2=\Sigma_{\{N_l\}}(N_l-n_l)^2|\psi_{\{N_l\}}|^2$, h is the matrix element of the hopping Hamiltonian, and $V_{\{N_l\}}=\Sigma_l(U_lN_l+GN_l^2)$ is the potential energy. When there is no hopping term ($h=0$), an exact solution to this equation as a product of Gaussian-like wave functions is written as

$$\psi_{\{N_l\}}(t)=\exp(i\varphi_{\{N_l\}})\exp\left(-\frac{i}{\hbar}V_{\{N_l\}}t\right)\times\prod_l\frac{1}{[2\pi\sigma_l^2(t)]^{1/4}}\exp\left(-\frac{[N_l-n_l(t)]^2}{4\sigma_l^2(t)}\right). \tag{22}$$

The population mean value per site $n_l(t)$ does a random walk, while its dispersion decreases as $\sigma_l^2(t)=\sigma_l^2(0)/[1+4\sigma_l^2(0)St]$. Here $\sigma_l^2(0)$ is the initial dispersion in the number of atoms per site, and it scales as N for an initial coherent state. Thus, the measurement drives the quantum state of the condensate to a Fock state. When tunneling between different lattice sites is allowed ($h\neq0$), localization in a Fock state is inhibited due to a competition between the measurement, which drives localization, and hopping, which tries to drive the state of the condensate towards coherent states. When measurement outweighs hopping, the final state of the BEC is a number squeezed state. The time scale in which squeezing is achieved is given by

$$t_{\mathrm{sq}}=\frac{1}{n_lS} \tag{23}$$

and the associated dispersion in the number of atoms per site for the asymptotic squeezed state is

$$\sigma_l=(\omega n_l/S)^{1/4}. \tag{24}$$

In a coherent state, the number fluctuations per site are Poissonian, $\sigma_l=n_l^{1/2}$. The state is squeezed when $(\omega n_l/S)^{1/4}<n_l^{1/2}$, i.e., sub-Poissonian atomic number fluctuations. This condition defines the strong measurement as

$$\frac{n_lS}{\omega}>1. \tag{25}$$

Number squeezing of a Bose condensate has been experimentally observed in an optical lattice in [31]. Our situation has an important difference from the latter case: since the squeezing is driven by the (Lindblad) measurement term, the evolution into such states is irreversible, even after removal of the imaging photon field. From this viewpoint, our squeezing technique is similar to the spin squeezing through quantum nondemolition measurements proposed in [32] and demonstrated in [33]. Of course, the system will eventually drift towards coherent, classical states due to the interaction with the external environment and the related decoherence [34], for instance due to the thermal component or residual background gas in the trapping volume.

IV. WEAK MEASUREMENT: STOCHASTIC GROSS-PITAEVSKII EQUATION

Unraveling the Lindblad equation derived above leads, in the limit of weak measurements, to a stochastic equation for the condensate wave function. In the mean-field approximation, this equation becomes the analog of the (deterministic) Gross-Pitaevskii equation for the unmeasured system. From Eqs. (10) and (11) and ignoring the depletion term $-L_2\rho$ we obtain a continuum version of the master equation,

$$\frac{d\rho}{dt}=-\frac{i}{\hbar}[H,\rho]-\int d^2r_1\times\int d^2r_2K(\mathbf{r}_1-\mathbf{r}_2)[n(\mathbf{r}_1),[n(\mathbf{r}_2),\rho]], \tag{26}$$

where H is the self-Hamiltonian of the system of N atoms in a 2D trap,

$$H=\int d^2r\left(-\frac{\hbar^2}{2m}\nabla\Psi^\dagger\nabla\Psi+U(\mathbf{r})\Psi^\dagger\Psi+\frac{g_{2D}}{2}\Psi^\dagger\Psi^\dagger\Psi\Psi\right). \tag{27}$$

A nonlinear stochastic (Itô) unraveling of the master equation (26) is

$$\begin{aligned} d|\Psi\rangle=&-\frac{i}{\hbar}dtH|\Psi\rangle \\ &-dt\int d^2r_1\int d^2r_2K(\mathbf{r}_1-\mathbf{r}_2)\Delta n(\mathbf{r}_1)\Delta n(\mathbf{r}_2)|\Psi\rangle \\ &+\int d^2r\,dW(\mathbf{r})\Delta n(\mathbf{r})|\Psi\rangle. \end{aligned} \tag{28}$$

Here $\Delta n(\mathbf{r})=n(\mathbf{r})-\langle\Psi|n(\mathbf{r})|\Psi\rangle$ and the Gaussian noises have correlators

$$\begin{aligned} \overline{dW(\mathbf{r})}&=0, \\ \overline{dW(\mathbf{r}_1)dW(\mathbf{r}_2)}&=2dtK(\mathbf{r}_1-\mathbf{r}_2). \end{aligned} \tag{29}$$

This unraveling corresponds to phase contrast measurement of the density of the condensate. The evolution of $|\Psi\rangle$ given by Eq. (28) describes a single realization of the experiment [23,35–37].

For a single atom, $N=1$, described by a wave function $\phi(t,\mathbf{r})=\langle\mathbf{r}|\Psi\rangle$, the stochastic Schrödinger equation takes the form

$$\begin{aligned} d\phi(\mathbf{r})=&-\frac{i}{\hbar}dt\left[-\frac{\hbar^2}{2m}\nabla^2+U(\mathbf{r})\right]\phi(\mathbf{r}) \\ &+\left[dW(\mathbf{r})-\int d^2r'|\phi(\mathbf{r}')|^2dW(\mathbf{r}')\right]\phi(\mathbf{r})+\mathcal{C}. \end{aligned} \tag{30}$$

The second term in brackets follows from the last term in Eq. (28), while the counterterm $\mathcal{C}$ comes from the second term on the right-hand side (RHS) of Eq. (28). The latter is necessary to conserve the norm $\int d^2r|\phi(\mathbf{r})|^2=1$, and it is given by

$$\begin{aligned} \mathcal{C}=dt\Big[&-K(0)+2\int d^2r_1K(\mathbf{r}-\mathbf{r}_1)|\phi(\mathbf{r}_1)|^2 \\ &-\int d^2r_1\int d^2r_2|\phi(\mathbf{r}_1)|^2K(\mathbf{r}_1-\mathbf{r}_2)|\phi(\mathbf{r}_2)|^2\Big]\phi(\mathbf{r}). \end{aligned} \tag{31}$$

This counterterm is highly nonlocal in $\phi(\mathbf{r})$. Fortunately, to implement the stochastic terms numerically one can use

$$\begin{aligned} d|\phi(\mathbf{r})|^2=&2\,dt\left[dW(\mathbf{r})-\int d^2r'|\phi(\mathbf{r}')|^2dW(\mathbf{r}')\right]|\phi(\mathbf{r})|^2 \\ &+\overline{\left[dW(\mathbf{r})-\int d^2r'|\phi(\mathbf{r}')|^2dW(\mathbf{r}')\right]^2}|\phi(\mathbf{r})|^2 \\ &+[\mathcal{C}\phi^*(\mathbf{r})+\text{c.c.}] \\ =&2\,dt\left[dW(\mathbf{r})-\int d^2r'|\phi(\mathbf{r}')|^2dW(\mathbf{r}')\right]|\phi(\mathbf{r})|^2, \end{aligned} \tag{32}$$

where the $\mathcal{C}$ was used to cancel out the average of the stochastic terms squared. The stochastic terms affect directly only the modulus of $\phi(\mathbf{r})$, so Eq. (32) is all that one needs to implement them. Note also that Eq. (32) manifestly conserves the norm.

Let us now analyze the case of an arbitrary number of atoms. For a weak measurement, when the squeezing of the quantum state is small, one can approximate the stochastic conditional state of N atoms in Eq. (28) by a product mean-field state,

$$\langle\mathbf{r}_1,\ldots,\mathbf{r}_N|\Psi\rangle=\prod_{i=1}^N\phi(\mathbf{r}_i), \tag{33}$$

with all the N atoms in the same condensate wave function $\phi(t,\mathbf{r})$. We assume that, under the evolution given by Eq. (28), the state of the N atoms remains in a product state Eq. (33) with a time-dependent $\phi(\mathbf{r},t)$. In order to derive a stochastic Gross-Pitaevskii (SGP) equation for the condensate wave function $\phi(\mathbf{r})$, we study the different terms in Eq. (28) separately. The stochastic term proportional to dW on the RHS of Eq. (28) involves only a one-body operator

$$\Delta n(\mathbf{r})\equiv n(\mathbf{r})-\langle\Psi|n(\mathbf{r})|\Psi\rangle=\sum_{k=1}^N\delta(\mathbf{r}-\mathbf{r}_k)-N\phi^*\phi(\mathbf{r}), \tag{34}$$

so the position representation of this term is the same as for the $N=1$ atom,

$$\left[dW(\mathbf{r})-\int d^2r'|\phi(\mathbf{r}')|^2dW(\mathbf{r}')\right]\phi(\mathbf{r}), \tag{35}$$

compare Eq. (30).

The contribution arising from the second term on the RHS of Eq. (28) for $N>1$ might be expected to be different from that corresponding to the $N=1$ case because the operator $\Delta n(\mathbf{r}_1)\Delta n(\mathbf{r}_2)$ contains a two-body operator $n(\mathbf{r}_1)n(\mathbf{r}_2)$, so that one could think it scales as N^2. However, the operator $\Delta n(\mathbf{r}_1)\Delta n(\mathbf{r}_2)$ is in fact much more weakly dependent on N. Indeed, in the weak measurement regime we are considering, the state of the condensate is described by a coherent state and therefore number fluctuations are well approximated by the Poissonian statistics. Hence, in the product state Eq. (33),

$\langle\Psi|\Delta n(\mathbf{r}_1)\Delta n(\mathbf{r}_2)|\Psi\rangle = O(N)$. The operator $\Delta n \Delta n$ scales with N like a one-body operator. Hence the contribution from this operator to the SGP equation is the same as for $N=1$. We can see this explicitly by calculating the position representation of the second term on the RHS of Eq. (28). First we ccompute the left-hand side of Eq. (28) using the ansatz Eq. (33). To order $O(dt)$, the change of the wave function is given by

$$d[\phi(\mathbf{r}_1)\cdots\phi(\mathbf{r}_N)] = \sum_{k=1}^{N} d\phi(\mathbf{r}_k)\prod_{m\neq k}\phi(\mathbf{r}_m) + \sum_{k\neq l}\overline{d\phi(\mathbf{r}_k)d\phi(\mathbf{r}_l)}\prod_{m\neq k,l}\phi(\mathbf{r}_m). \tag{36}$$

We use Eq. (35) and the correlator of the noises Eq. (29) to evaluate the noise averages in Eq. (36), and then we project the result onto $\phi^*(\mathbf{r}_1)\cdots\phi^*(\mathbf{r}_N)$. We define as L the resulting projection, which reads

$$L = N\int d^2r\ \phi^\star(\mathbf{r})d\phi(\mathbf{r}). \tag{37}$$

In a similar way, project the second term on the RHS of Eq. (28) onto $\phi^\star(\mathbf{r}_1)\cdots\phi^\star(\mathbf{r}_N)$. We call R the result,

$$\begin{aligned} R &= -dt\int d^2r_1\phi^*\phi(\mathbf{r}_1)\cdots\int d^2r_N\phi^*\phi(\mathbf{r}_N) \\ &\times\int d^2r'\int d^2r''K(\mathbf{r}'-\mathbf{r}'')\left[\sum_{k=1}^{N}\delta(\mathbf{r}_k-\mathbf{r}') - N\phi^*\phi(\mathbf{r})\right]\left[\sum_{l=1}^{N}\delta(\mathbf{r}_l-\mathbf{r}'') - N\phi^*\phi(\mathbf{r})\right] \\ &= -Ndt\,K(0)\int d^2r\ \phi^*(\mathbf{r})\phi(\mathbf{r}) \\ &+ Ndt\int d^2r'\int d^2r''p(\mathbf{r}')K(\mathbf{r}'-\mathbf{r}'')p(\mathbf{r}''), \end{aligned} \tag{38}$$

where $p(r)=\phi^*(r)\phi(r)$. As we can see, $R=O(N)$ just like $L=O(N)$, and there are no two-body terms $O(N^2)$. Comparing L/N with R/N, we see that $d\phi(\mathbf{r})$ is given by an expression that does not depend on N. Hence, as we have already mentioned, the measurement terms in the stochastic Gross-Pitaevskii equation are the same as in the stochastic Schrödinger equation for $N=1$.

Finally, we derive this interaction term in the same way as we derived the measurement term. In the position representation, we project the interaction term $(g_{2D}/2)\Psi^\dagger\Psi^\dagger\Psi\Psi|\Psi\rangle$ contained in $H|\Psi\rangle$ in Eq. (28) onto $\phi^*(\mathbf{r}_1)\cdots\phi^*(\mathbf{r}_N)$ and obtain

$$R_{\rm int} = -\frac{i}{\hbar}g_{2D}N(N-1)\int d^2r\ \phi^*\phi^*\phi\phi = O(N^2). \tag{39}$$

Again, comparing L/N with $R_{\rm int}/N$ we get the interaction term.

The final expression for the Itô SGP equation reads

$$\begin{aligned} d\phi(\mathbf{r}) &= -\frac{i}{\hbar}dt\left[-\frac{\hbar^2}{2m}\nabla^2 + U(\mathbf{r}) + (N-1)g_{2D}|\phi(\mathbf{r})|^2\right]\phi(\mathbf{r}) \\ &+ \left[dW(\mathbf{r}) - \int d^2r'|\phi(\mathbf{r}')|^2 dW(\mathbf{r}')\right]\phi(\mathbf{r}) + \mathcal{C}. \end{aligned} \tag{40}$$

The only difference with respect to the case of $N=1$, compare Eq. (30), is the usual interaction term $(N-1)g_{2D}|\phi(\mathbf{r})|^2$.

As a final remark, we mention that stochastic nonlinear Schrödinger equations have been proposed and studied for a quite different goal, namely to describe single trajectories through unraveling of the exact N-body quantum evolution of a boson system [38]. In the latter case, the interpretation of the underlying stochasticity is obtained in terms of the randomness attributable to each quantum trajectory, to be confronted with the stochasticity that in our case is instead due to the opening of the condensate to a particular environment, namely the measurement apparatus.

V. SGP EQUATION VERSUS EXACT QUANTUM EVOLUTION: MEASUREMENTS IN A DOUBLE WELL

In this section, we want to test the validity of the SGP equation in a significant but simple situation. To this end, we consider the double-well problem in the two-mode approximation, and compare the quantum dynamics including the measurement backaction with the dynamics given by the SGP equation. The Hamiltonian of the model is

$$H = \epsilon(a_1^\dagger a_1 + a_2^\dagger a_2) - \hbar\omega(a_1^\dagger a_2 + a_2^\dagger a_1) + \frac{G}{2}[(a_1^\dagger)^2a_1^2 + (a_2^\dagger)^2a_2^2], \tag{41}$$

where ϵ is the mode frequency (assumed to be the same for both modes), ω is the tunneling angular frequency, and G is the two-particle interaction strength. We perform phase-contrast imaging on each site, and we assume that the kernel resolution is much shorter than the distance between sites, so that there is no cross term due to the measurement. The Itô version of the stochastic Schrödinger equation for the state ket reads

$$\begin{aligned} d|\Psi_Q\rangle &= dt\left[-\frac{i}{\hbar}H - \frac{S}{2}(n_1-\langle n_1\rangle)^2 - \frac{S}{2}(n_2-\langle n_2\rangle)^2\right]|\Psi_Q\rangle \\ &+ dW_1(n_1-\langle n_1\rangle)|\Psi_Q\rangle + dW_2(n_2-\langle n_2\rangle)|\Psi_Q\rangle, \end{aligned} \tag{42}$$

where the noise satisfies $\overline{dW_\alpha}=0$ and $\overline{dW_\alpha dW_\beta}=2K_{\alpha\beta}dt$, with $\alpha,\beta=1,2$, and $K_{\alpha\beta}=S\delta_{\alpha\beta}$ is the measurement kernel.

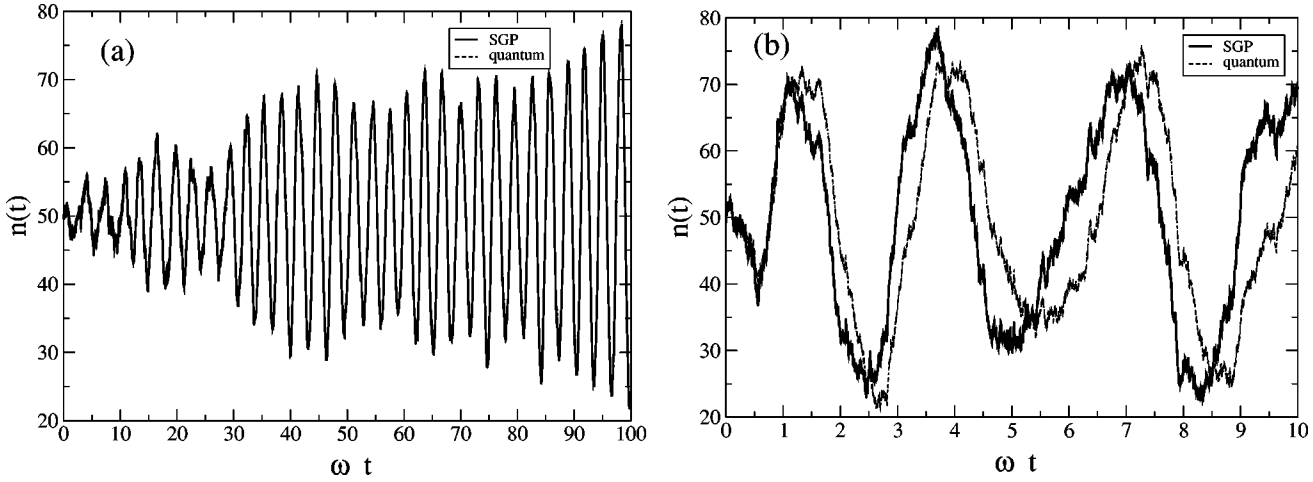

FIG. 1. Comparison between the SGP and the exact quantum evolution for weak measurements on a noninteracting Bose condensate. The population $n(t)$ in a given well is plotted as a function of time for a single stochastic realization, expressed in units of cycles of the Rabi oscillations. The total number of particles is $N=100$. (a) The SGP evolution and the quantum one coincide for an effective measurement strength $nS/\omega=10^{-1}$ even for times much greater than $1/nS=10/\omega$. (b) The departure of the SGP dynamics from the exact one at the time $1/nS=1/\omega$ is evident for a stronger measurement coupling $nS/\omega=1$.

By assuming a total of N atoms, distributed between the two sites, $N=N_1+N_2$, we can expand the state in terms of Fock states at each well,

$$|\Psi_Q\rangle=\sum_{k=0}^{N}\psi_k(t)|k,N-k\rangle. \tag{43}$$

We solve numerically the corresponding equation for the coefficients $\psi_k(t)$ starting from a mean-field state with equal mean populations in each well, $|\Psi\rangle_{t=0}=(1/\sqrt{N!})[(1/\sqrt{2})a_1^\dagger+(1/\sqrt{2})a_2^\dagger]^N|0\rangle$. The equation provides us with the full quantum evolution including the measurement backaction. We want to compare it with the one that results from the stochastic GP equation. The GP state is

$$|\Psi_{\mathrm{GP}}\rangle=\frac{1}{\sqrt{N!}}[\phi_1(t)a_1^\dagger+\phi_2(t)a_2^\dagger]^N|0\rangle, \tag{44}$$

where the wave functions ϕ_1 and ϕ_2 satisfy the following set of Itô SGP equations, which follow from Eqs. (31) and (40):

$$\begin{aligned}
d\phi_1=&-\frac{i}{\hbar}dt\{[\epsilon+(N-1)G|\phi_1|^2]\phi_1-\omega\phi_2\}\\
&+dW_1(1-|\phi_1|^2)\\
&+Sdt[-1+2|\phi_1|^2-(|\phi_1|^4+|\phi_2|^4)],\\
d\phi_2=&-\frac{i}{\hbar}dt\{[\epsilon+(N-1)G|\phi_2|^2]\phi_2-\omega\phi_1\}\\
&+dW_2(1-|\phi_2|^2)\\
&+Sdt[-1+2|\phi_2|^2-(|\phi_1|^4+|\phi_2|^4)],
\end{aligned} \tag{45}$$

and we take the same initial state as in the quantum evolution, namely a coherent state $\phi_1(0)=\phi_2(0)=1/\sqrt{2}$ with balanced populations $n_1(0)=n_2(0)$. In Fig. 1, we compare the time evolution of the quantum and SGP mean populations in one well. In these simulations, the total number of particles was $N=100$, and the nonlinear self-coupling was $G=0$. In this case, the Hamiltonian involves only one-body terms, so the mean-field evolution (based on coherent states) must exactly coincide with the quantum one for the case of zero measurement ($S=0$). For small measurement strengths, $nS/\omega\ll 1$ (here n denotes the average number of particles per site), the quantum state of the condensate is still, to a high degree of accuracy, a coherent state, so the SGP evolution and the quantum one coincide. In Fig. 1(a), we see that the agreement is good even for times much larger than $1/nS$. This time scale is relevant for the strong measurement case of the previous section, since it sets the time after which an asymptotic number squeezed state is reached. As we increase the measurement strength and reach $nS/\omega\geqslant 1$ [see Fig. 1(b)], the mean number of particles per well given by the SGP and the quantum evolution depart appreciably. This is not surprising since such strong measurements squeeze the quantum state of the condensate, driving it outside the description in terms of coherent states, i.e., the associated basis for the Gross-Pitaevskii equation.

The Gross-Pitaevskii evolution can depart from the quantum one not only due to the measurement backaction but also due to the nonlinearity of the interactions. In Fig. 2(a), we show the SGP and quantum evolutions for $S/\omega=10^{-3}$ and $G/\omega=10^{-3}$, corresponding to the same initial state as in previous figures. We see that the inclusion of the nonlinearity causes the SGP evolution to depart from the quantum one. To gain further insight, we introduce a quantity which measures the depleted fraction of atoms from the *best* mean-field state, i.e., a mean-field state that is the closest to the exact quantum state. Its definition is

$$D=\min_{\{A,\phi\}}\left(1-\frac{1}{N}\langle\Psi_Q|c^\dagger c|\Psi_Q\rangle\right), \tag{46}$$

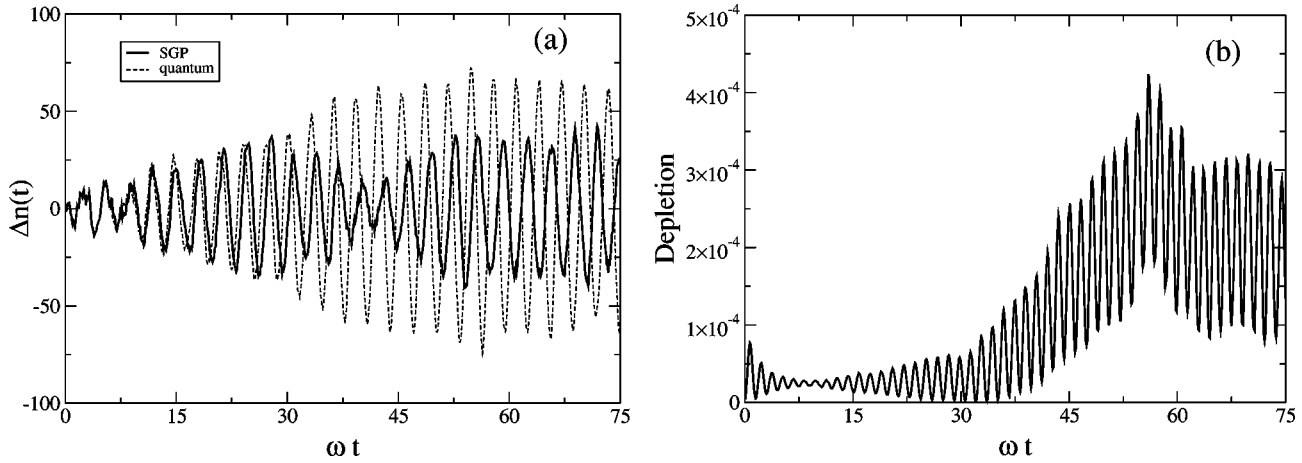

FIG. 2. Comparison between the SGP and the exact quantum evolution for a weakly interacting ($G/\omega = 10^{-3}$) Bose condensate subjected to a weak measurement $nS/\omega = 510^{-2}$. (a) The population difference $\Delta n(t) = n_2(t) - n_1(t)$ is plotted for a single stochastic realization. Initially the condensate is in a coherent state with equal populations in each mode, $n_1(0) = n_2(0) = 50$. (b) Depletion from a mean-field state for the same realization as in (a).

where the operator c is $c = \sqrt{A}a_1 + e^{i\phi}\sqrt{1-A^2}a_2$. In Fig. 2(b), we plot this depletion for the same simulation of Fig. 2(a). The depletion in Fig. 2(b) is small (less than one atom is depleted from the condensate), but, as we see in Fig. 2(a), the SGP evolution departs from the exact evolution. This departure is attributable to the inclusion of the nonzero G.

In Fig. 3(a), we show the GP and quantum evolution for $S = 0$ and $G/\omega = 10^{-3}$. Since no measurements are performed, an initial balanced population $[n_1(0) = n_2(0)]$ would remain balanced for all times, both at the GP and quantum level. For this reason, we take an initial unbalanced population, $n_1(0)/n_2(0) = \frac{3}{2}$, which due to the hopping term triggers Rabi oscillations between the two wells (just as the measurement did when we took initial balanced populations). It follows from the figure that the GP dynamics departs from the quantum one. We plot in Fig. 3(b) the depletion corresponding to Fig. 3(a). Again, this depletion remains small (less than one atom is depleted from the condensate).

As we can see in Figs. 2 and 3, both the SGP and GP evolutions depart from the exact evolution even in the weak measurement and interaction limits when the depletion from the condensate is small. The derivation of the backaction terms in the SGP equation requires only one assumption, namely that all the atoms are in the condensate. In contrast, the derivation of the interaction terms (both for SGP and GP equations) not only assumes that all the atoms are in the condensate but also makes further approximations to describe the evolution of the condensate wave function ϕ. This is why $G \neq 0$ causes both the SGP and GP evolutions to depart from the exact quantum evolution even for negligible depletion. However, even after the departure, the SGP and GP evolutions remain qualitatively similar to the exact evolution, see Figs. 2(a) and 3(a).

To summarize, the accuracy of the SGP equation is limited by the weak measurement condition, $nS/\omega < 1$, and by the nonlinear interaction. For a weak measurement, the ac-

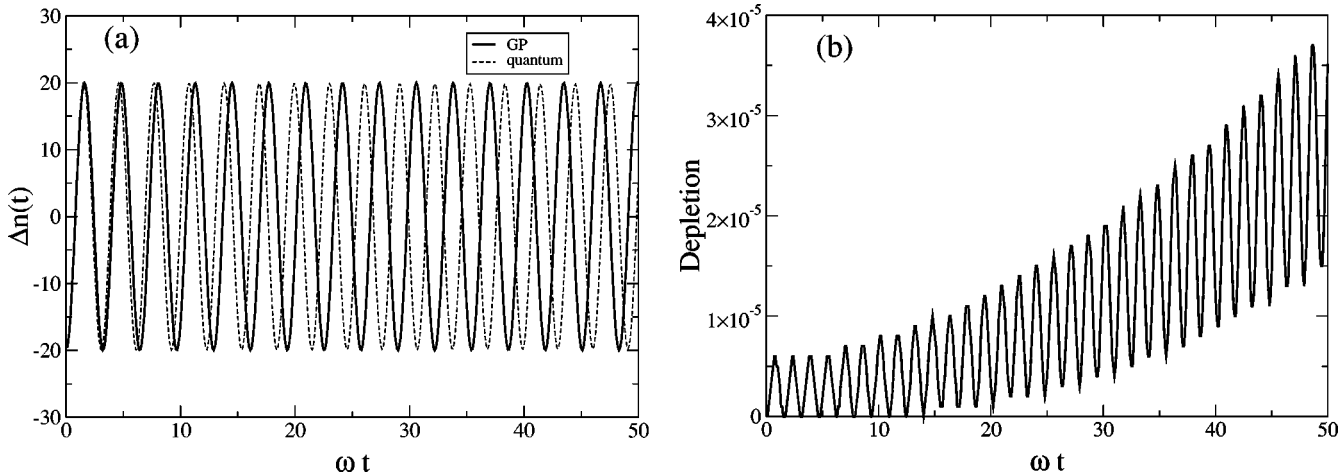

FIG. 3. Comparison between the standard GP and the exact quantum evolution for a weakly interacting ($G/\omega = 10^{-3}$) unmeasured Bose condensate. (a) The population difference $\Delta n(t) = n_2(t) - n_1(t)$ is plotted as a function of time. Initially the condensate is in a coherent state with unbalanced populations, $n_1(0) = 60$, $n_2(0) = 40$. (b) Depletion from a mean field state for the same realization as in (a).

curacy of the SGP equation is the same as that of the GP equation. In the next section, we apply the SGP equation to show how the measurement can trigger the unwinding of a dark soliton [39,40] in a realistic experimental setup.

VI. MEASUREMENT-INDUCED UNWINDING OF A DARK SOLITON

Once we delimit the validity of the stochastic Gross-Pitaevskii equation in the simple situation of a two-mode system, we can apply it to the more complex case of imaging of a condensate state with a nontrivial phase such as a soliton. Even in the limit of weak measurement, with the solution still approximable in terms of Gross-Pitaevskii coherent states, the effect of the measurement is present and affects the observable conjugate to the atom number, i.e., the phase of the condensate. As an example of application of the SGPE, let us consider an isotropic harmonic 2D trapping potential $V(\mathbf{r})=(m\Omega^2/2)(x^2+y^2)$. The condensate is assumed to be in the Thomas-Fermi limit of strong repulsive interaction, where the ground-state wave function can be well approximated by

$$\phi_{\mathrm{GS}}(\mathbf{r})=\sqrt{\frac{\mu-V(\mathbf{r})}{Ng_{2\mathrm{D}}}}. \tag{47}$$

The constant $\mu=\Omega\sqrt{Ng_{2\mathrm{D}}m/\pi}$, the chemical potential, is chosen so that the wave function is normalized to 1. Let us use as the initial state a dark soliton [39] imprinted on the Thomas-Fermi ground state,

$$\phi(t=0,\mathbf{r})=\tanh\left(\frac{x}{l}\right)\sqrt{\frac{\mu'-V(\mathbf{r})}{Ng_{2\mathrm{D}}}}. \tag{48}$$

Here l is the healing length at the peak density in the ground state (47).

In our numerical simulations, we assume the following parameters relevant for ^{87}Rb: mass $m=1.4\times10^{-25}$ kg, scattering length $a=5.8$ nm, $\chi_0=10^{-23}$ m^3, and wavelength $\lambda=780$ nm. The width of the Gaussian $\Lambda(z)$ is assumed to be $\xi=10$ μm and the healing length $l=0.6$ μm. With these parameters, the resolution of the kernel is $\Delta r=5$ μm. We assume a 2D harmonic trap frequency $\Omega=2\pi\times10$ s^{-1}. With $N=5\times10^5$, we get a 2D Thomas-Fermi radius of 31 μm. We also assume a laser intensity of $I=10^{-4}$ mW/cm^2.

The former parameters give a weak measurement strength in the sense discussed in Secs. III and IV, so that the use of the SGP equation is justified. Indeed, this continuous problem can be mapped on the lattice model, Eq. (20), where the lattice constant is the kernel resolution Δr. Given the Thomas-Fermi radius of 31 μm, and $\Delta r=5$ μm, we estimate the lattice to be composed of 100 sites with an average of $n=5000$ atoms per site. The measurement strength is equal to $S=7\times10^{-5}$ s^{-1} and the effective hopping frequency for the lattice model is $\omega=14$ s^{-1}. Therefore, $nS/\omega\approx2\times10^{-2}\ll1$, thus confirming a weak measurement regime.

To simulate the continuum SGP equation (40), we discretized it using a lattice constant 2π times smaller than the kernel resolution Δr. The program uses a split-step method: the fast Fourier transform was used to carry out the time integration of the kinetic term and of the nonlocal terms involving the kernel, and the potential and nonlinear coupling terms were integrated in time in the position representation. A cross section along the x axis through the probability density of the initial state (48) is shown in (a) of Fig. 4. Cross sections through probability densities at later times after the probe light beam has been sent on the condensate are shown in cases (b) and (c) of Fig. 4. For comparison, the time evolution without the measurement does not result in any soliton unwinding.

The soliton unwinds after roughly 50 ms. This time is much shorter than the depletion time $t_2=10^4$ s discussed at the end of Sec. II. The measurement induces soliton unwinding much earlier than any detectable depletion of atoms occurs. Figure 4 suggests that the unwinding will manifest itself by filling up the soliton core with atoms. Such a graying of the dark soliton can also occur through a different mechanism that involves collisions between condensate atoms. In Ref. [41], it was demonstrated that the dark soliton can gray on a time scale of tens of ms because its core fills up with noncondensed atoms (quantum) depleted from the condensate as a result of atomic collisions between condensed atoms. This is supported by recent results showing that the depleted atoms are strongly concentrated in the soliton core [42]. This quantum depletion process does not unwind the

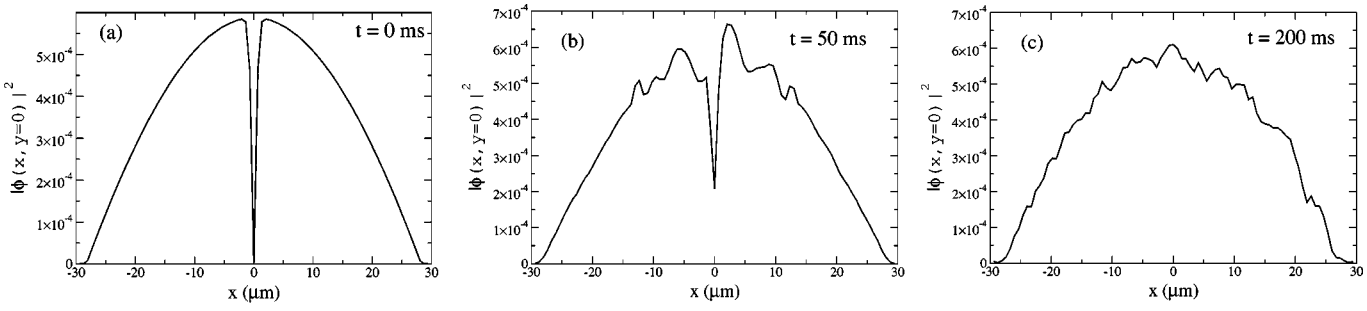

FIG. 4. Soliton unwinding during a continuous imaging. The figures show the cross section of the 2D probability density $|\phi(x,y)|^2$ of the Bose condensate along the x axis at $t=0$ ms (a), $t=50$ ms (b), and $t=200$ ms (c) since the beginning of the continuous imaging for a single realization solved through the SGP. The dark soliton is graying progressively and in the third profile there is no trace of the initially imprinted pattern. The laser intensity is $I=10^{-4}$ mW/cm^2, and the condensate wave function is normalized to unity in 2D.

soliton: the condensate remains in the soliton state with a phase jump of π. The phase jump or its unwinding could be detected by interference between two condensates, one of them in a ground state and the other with a soliton [43]. A simpler way to verify that the observed graying is due to the measurement-induced unwinding is to change the measurement strength in a certain range and see if the graying time depends on the imaging laser intensity. We simulated the soliton unwinding for a range of measurement strengths. Figure 5 shows the unwinding time τ versus the laser intensity I. The time τ is defined as that for which the density at $x=0$ in Fig. 4 achieves 10% of the maximal density. Similar considerations can also be applied to the phase scrambling of a vortex state. Thus, analogous to finite-temperature effects on the vortex lifetime studied in [17], one could study zero-temperature vortex lifetimes due to the continuous measurement process.

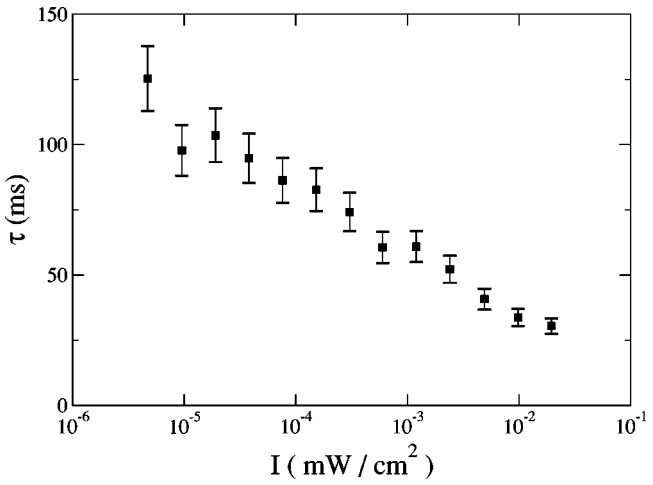

FIG. 5. Average unwinding time τ as a function of the laser intensity I. Each point is an average over ten single stochastic realizations. The point corresponding to the highest value for the intensity is still within the weak measurement limit.

VII. CONCLUSIONS

Quantum measurement theory has been applied to the dispersive imaging of a Bose-Einstein condensate. In the strong measurement limit, the condensate is irreversibly driven into nonclassical states with reduced number fluctuations. In the opposite limit of weak measurement, the condensate can be approximately described for short time scales through a stochastic counterpart of the Gross-Pitaevskii equation. The latter has been applied for the study of the dynamics induced by dispersive imaging on a condensate prepared in a soliton state. The proposed model, besides allowing to intentionally design selective manipulation of the condensate state (for instance to quench vortices without introducing appreciable depletion), could also lead to a better understanding of quantum phase transitions [44,45] in Bose condensates [46,47].

ACKNOWLEDGMENTS

We would like to thank Ivan Deutsch for calling our attention to Refs. [32,33], and Zbyszek Karkuszewski for helping us with the numerical simulations. D.D. was supported in part by NSA and J.D. was supported in part by NSA and KBN Grant No. 5 P03B 088 21.

[1] *Quantum Theory and Measurement,* edited by J. A. Wheeler and W. H. Zurek (Princeton University Press, Princeton, NJ, 1983).
[2] V. B. Braginsky and F. Ya. Khalili, *Quantum Measurements* (Cambridge University Press, Cambridge, 1992).
[3] C. Santarelli *et al.*, Phys. Rev. Lett. **82**, 4619 (1999).
[4] For a review, see W. Ketterle, D. S. Durfee, and D. M. Stamper-Kurn, in *Bose-Einstein Condensation in Atomic Gases*, Proceedings of the International School of Physics "Enrico Fermi," Course CXL, Varenna, 1998, edited by M. Inguscio, S. Stringari, and C. Wieman (IOS Press, Amsterdam, 1999).
[5] D.G. Fried *et al.*, Phys. Rev. Lett. **81**, 3811 (1998).
[6] W. Pauli, *General Principles in Quantum Mechanics* (Springer, Berlin, 1980) [*Die Allgemeinen Prinzipien der Wellenmechanik,* edited by H. Geiger and K. Schoeel, Handbuch der Physik Vol. XXIV (Springer-Verlag, Berlin, 1933)].
[7] M.R. Andrews *et al.*, Science **273**, 84 (1996).
[8] V. Savalli *et al.*, Opt. Lett. **24**, 1552 (1999).
[9] J.E. Lye, B.D. Cuthbertson, H.-A. Bachor, and J.D. Close, J. Opt. B: Quantum Semiclassical Opt. **1**, 402 (1999).
[10] S. Kalecek, J. Sebby, R. Newell, and T.G. Walker, Opt. Lett. **26**, 137 (2001).
[11] C.A. Sackett, C.C. Bradley, M. Welling, and R.G. Hulet, Braz. J. Phys. **27**, 154 (1997).
[12] H.J. Miesner *et al.*, Science **279**, 1005 (1998).
[13] M.R. Andrews *et al.*, Phys. Rev. Lett. **80**, 2967 (1998).
[14] D.M. Stamper-Kurn *et al.*, Phys. Rev. Lett. **81**, 500 (1998).
[15] R. Onofrio *et al.*, Phys. Rev. Lett. **85**, 2228 (2000).
[16] M.R. Matthews *et al.*, Phys. Rev. Lett. **83**, 2498 (1999).
[17] J.R. Abo-Shaeer *et al.*, Phys. Rev. Lett. **88**, 070409 (2002).
[18] C.M. Caves, K.S. Thorne, R.W.P. Drever, V.D. Sandberg, and M. Zimmermann, Rev. Mod. Phys. **52**, 341 (1980).
[19] M.F. Bocko and R. Onofrio, Rev. Mod. Phys. **68**, 755 (1996).
[20] D. A. R. Dalvit, J. Dziarmaga, and R. Onofrio, Phys. Rev. A **65**, 033620 (2002).
[21] J. Ruostekoski and D.F. Walls, Phys. Rev. A **56**, 2996 (1997); **58**, R50 (1998); **59**, R2571 (1999).
[22] J.F. Corney and G.J. Milburn, Phys. Rev. A **58**, 2399 (1998).
[23] H. J. Carmichael, *An Open Systems Approach to Quantum Optics* (Springer, Berlin, 1993).
[24] M.R. Andrews *et al.*, Science **275**, 637 (1997).
[25] A. Görlitz *et al.*, Phys. Rev. Lett. **87**, 130402 (2001).
[26] R. Onofrio and L. Viola, Phys. Rev. A **58**, 69 (1998).
[27] C.F. Li and G.C. Huo, Phys. Lett. A **248**, 117 (1998).
[28] U. Leonhardt, T. Kiss, and P. Piwnicki, Eur. Phys. J. D **7**, 413 (1999).

[29] H.M. Wiseman and L.K. Thomsen, Phys. Rev. Lett. **86**, 1143 (2001).
[30] D.A.R. Dalvit, J. Dziarmaga, and W.H. Zurek, Phys. Rev. Lett. **86**, 373 (2001).
[31] C. Orzel *et al.*, Science **291**, 2386 (2001).
[32] A. Kuzmich, N.P. Bigelow, and L. Mandel, Europhys. Lett. **42**, 481 (1998); A. Kuzmich *et al.*, Phys. Rev. A **60**, 2346 (1999).
[33] A. Kuzmich, L. Mandel, and N.P. Bigelow, Phys. Rev. Lett. **85**, 1594 (2000).
[34] W.H. Zurek, Phys. Today **44(10)**, 36 (1991); D.A.R. Dalvit, J. Dziarmaga, and W.H. Zurek, Phys. Rev. A **62**, 13 607 (2000); J.R. Anglin, Phys. Rev. Lett. **79**, 6 (1997).
[35] H.M. Wiseman and G.J. Milburn, Phys. Rev. Lett. **70**, 548 (1993); H. M. Wiseman, Ph.D. thesis, University of Queensland, 1994.
[36] D. Gatarek and N. Gisin, J. Math. Phys. **32**, 2152 (1991); N. Gisin and J.C. Percival, J. Phys. A **26**, 2233 (1993); I. Percival, *ibid.* **27**, 1003 (1994).
[37] M.B. Plenio and P.L. Knight, Rev. Mod. Phys. **70**, 101 (1998).
[38] P.D. Drummond and J.F. Corney, Phys. Rev. A **60**, R2661 (1999); I. Carusotto, Y. Castin, and J. Dalibard, *ibid.* **63**, 023606 (2001).
[39] S. Burger *et al.*, Phys. Rev. Lett. **83**, 5198 (1999); J. Denschlag *et al.*, Science **287**, 97 (2000).
[40] A.E. Muryshev *et al.*, Phys. Rev. A **60**, 2665 (1999); P.O. Fedichev *et al.*, *ibid.* **60**, 3220 (1999); Th. Busch and J.R. Anglin, Phys. Rev. Lett. **84**, 2298 (2000).
[41] J. Dziarmaga, Z. Karkuszewski, and K. Sacha, cond-mat/0110080.
[42] C.K. Law, P.T. Leung, and M.-C. Chu, e-print cond-mat/0110428.
[43] S. Inouye *et al.*, Phys. Rev. Lett. **87**, 080402 (2001); F. Chevy, K.W. Madison, V. Bretin, and J. Dalibard, Phys. Rev. A **64**, 031601(R) (2001).
[44] M.P.A. Fisher, P. Weichman, G. Grinstein, and D.S. Fisher, Phys. Rev. B **40**, 546 (1989).
[45] S. Sachdev, *Quantum Phase Transitions* (Cambridge University Press, New York, 2000).
[46] D. Jaksch *et al.*, Phys. Rev. Lett. **81**, 3108 (1998).
[47] M. Greiner, O. Mandel, T. Esslinger, T.W. Hänsch, and I. Bloch, Nature (London) **415**, 39 (2002).